Anomalies in above-threshold ionization observed in H_2 and its excited fragments

J. W. J. Verschuur, L. D. Noordam, and H. B. van Linden van den Heuvell
Fundamenteel Onderzoek der Materie-Institute for Atomic and Molecular Physics, Kruislaan 407, 1098 SJ Amsterdam, The Netherlands
(Received 3 April 1989)

The photoelectron energy spectra resulting from a multiphoton process in H_2 with high laser intensities is, in general, determined by the character of the intermediate resonance state. Above-threshold ionization (ATI) is observed in the ionization of the molecule H_2 as well as of its excited atomic fragments, and even of atomic hydrogen in the ground state. ATI is observed with five, three, and two extra photons for three different wavelengths $\lambda=532$ nm, $\lambda=355$ nm, and $\lambda=266$ nm, respectively. In the $\lambda=532$ nm spectra radiative coupling between dressed states is observed. A shift to higher values of the center of the vibrational distribution of the ion by seven vibrational quanta is observed between ATI peaks which differ by four photon energies. A calculation, taking into account a coupling of the $B\,^1\Sigma_u^+$ state to the dressed $^1\Sigma_g^+(2p\sigma_u)^2$ state, and of the $X\,^2\Sigma_g^+$ state by the dressed $2p\sigma_u$ state, shows the trend of the observed ionization spectrum. The calculation is performed to describe the effect on the average of the vibrational distribution and not on the distribution itself. The structure of the ATI spectrum in the $\lambda=355$ nm and $\lambda=266$ nm is nearly a reproduction of the normal ionization spectrum, repeated several times at higher electron energies. In the $\lambda=266$ nm spectra both ATI of the molecule, as well as ATI of the atomic fragments, are observed.

I. INTRODUCTION

In contrast with atoms, the study of molecules in intense radiation fields is a relatively unexplored area of research. Extensive studies are made of above-threshold ionization (ATI) of atoms, experimentally mainly on xenon, and theoretically mainly on hydrogen. This work was initiated by the experimental results of Agostini *et al.*[1] and Kruit *et al.*[2] However, experimental data of above-threshold ionization in molecules is rather scarce. The only experimental data available at the moment are the ATI spectra of H_2 reported by Morellec and coworkers.[3,4] In their photoelectron spectra, one excess photon is absorbed in the various vibrational ionization continua. Also, the group of Bucksbaum and coworkers[5] is working on this subject. An effect closely related to ATI is observed by Miller ad Compton,[6] and Kimman *et al.*[7] in the photoelectron spectrum of NO. Both report four-photoionization to high vibrational levels of the ionic ground state, while the lower vibrational levels were already accessible with three photons. More recently, this is also observed in H_2 by Verschuur *et al.*[8]

The attraction of studying ATI in molecules is that molecular parameters, which are not present in the atomic processes have an impact on ATI. In particular, the fact is that electronic potentials are dependent on the internuclear distance. This means that radiative couplings between two electronic potentials are localized, with respect to the internuclear distance. Obviously, this has a large impact on the vibrations of the molecule in the perturbed potentials. Since the vibrational wave functions of an intermediate state determine the vibrational distribution of the ionic ground state, a change in these wave functions causes a change in the population of the vibrational ionization continua. In this way, part of the excess photon energy can go to the vibrational motion of the ion, and is not necessarily converted to electron energy. Since there are more exit channels involved, also characteristic molecular time scales can become important in the evolution of the observed processes.

Only recently it has been recognized that with intense laser fields it is possible to vary the strength of the coupling between electronic states, and thus to manipulate the dynamics. Recently, Normand and Morellec[9] observed a change in the competition between photoionization and predissociation in H_2, as a function of the intensity of radiation field. Bigio *et al.*[10,11] presented intensity effects on the Franck-Condon distribution of a resonantly enhanced multi-photon ionization (REMPI) process due to a mixing with dissociative intermediate states. Several theories[12–14] are developed to describe molecules in an intense laser field. These theories are based on the "dressed-state" model, which originates from the description of the ac Stark shift of atomic levels due to the intense radiation field.[15] In molecules, the ac Stark shift is more complicated, since the mixing of electronic states is not only dependent on the light intensity but also on the internuclear distances. The molecular dressed-state theories are applied to the photodissociation of the diatomic molecular ions H_2^+ (Ref. 13) and Ar_2^+.[12] The effect of moderate radiation field strengths is reported in experiments of Quesada *et al*,[16] in which the ac Stark splitting in the multiphoton ionization of H_2 is measured in a two-color, double-resonance technique, where the ac Stark shift induced by the first laser is monitored by a second, weaker laser.

The observation of ATI peaks in a photoelectron energy spectra is an indication that the radiative couplings

 ©1989 The American Physical Society

between states cannot be neglected in describing the observed results. Analogous to ATI in atoms, ATI in molecules can be described by the dressed-state model, in which the various ATI peaks are the redistribution of the photon states and the molecular ion states. Observation of more than one ATI peak is an indication that also coupling between bound states that are dressed by more than one photon become important. For a complete description of the observed features the need for an elaborate theory treating the full dressed-state picture with all electronic couplings included is unavoidable.

In this paper we report a multiphoton ionization photoelectron spectroscopy (MPI PES) study on H_2 with laser intensities in the order of 10^{13} W/cm^2. Photoelectron energy spectra are recorded with various harmonics of a Nd:YAG laser (YAG denotes yttrium aluminum garnet). Evidently, the harmonics of the Nd:YAG laser are chosen for the high intensities available. The initial nonresonant multiphoton ionization at these wavelengths is essential to avoid saturation of the process at relative low intensities. In describing the ATI spectra we are restricted to a preliminary qualitative description, only indicating the dominant interactions.

II. EXPERIMENT

The experiments reported here are performed with a mode-locked Nd:YAG laser as a picosecond light source to perform the multiphoton ionization process, and a magnetic-bottle photoelectron spectrometer to analyze the energy of the electrons after ionization. The Nd:YAG laser is equipped with an acousto-optic modulator running at 70 MHz and mode-locked with the dye Q-switch I. The pulse slicer is positioned outside the oscillator. The pulse is amplified in a double-pass amplifier. The resulting output is a laser pulse of 10 mJ at $\lambda=1064$ nm, and a pulse duration of 35 ps. The pulses are nearly bandwidth limited which corresponds to a bandwidth somewhat larger than 0.4 cm^{-1}. The pulses are produced at a frequency of 30 Hz. For the different experiments different harmonics of the fundamental frequency are used. These harmonics are generated in potassium dihydrogen phosphate (KDP) crystals in various configurations. A Pellin-Broca prism is used to select the desired wavelength for the experiment. The pulse energy is varied by adjusting the voltage on the flash-lamps of the amplifier in a regime of stable operation. The laser beam is focused in the spectrometer by a lens with a focal distance of 25 mm. The intensities given in this paper are calculated from the pulse energy, the pulse duration, and the focus diameter. The focus diameter is calculated, taking into account the spherical aberration and the diffraction limitation.

The magnetic-bottle spectrometer with a 2π-sr acceptance angle for the electrons is described elsewhere.[17] Time-of-flight (TOF) spectra are recorded at various retarding field values. The high-resolution parts of the TOF spectra are transformed and reconstructed to an energy spectrum. The spectrometer is normally filled with H_2 at a pressure of 7 mPa with a background pressure of 27 μPa. This value is the optimum between a high pressure to optimize the H_2-signal to background-signal ratio, and a low pressure to minimize space-charge effects. The H_2-signal to background-signal ratio is a serious problem since the excitation in H_2 is not necessarily a resonant process, and the ionization potential of H_2 is higher than the ionization potential of most of the background species. The need for high intensities in combination with the high H_2-signal to background ratio gives rise to the problem of space charge in the focus. For the highest intensities used, it was not possible to avoid an error in the energy axis below 4 eV due to space charge. The amount of signal at the highest intensities was that large that even the channel-plate detector ran into saturation. To avoid the saturation of the channel-plate detector, the voltage on the channel plates was reduced when the TOF spectra with the low retarding voltages were recorded. Some of the electron energy spectra are therefore a construction of two sets of TOF spectra, recorded with different channel-plate voltages. Obviously, this does not reduce the space charge. The resolution and the overall accuracy of the photoelectron energy spectra is about 20 and 100 meV, respectively.

III. EXCITATION SCHEMES

Although most excitations presented in this paper are initially nonresonant, it is useful to indicate the position of the intermediate resonances for each wavelength in the potential diagram of H_2. Due to the field-induced shift, nearby states may shift into resonance. Effectively, a band of energies can be excited in the molecule in this way. We call these bands excitation regions. The potential diagrams are a first step to unravel the measured photoelectron spectra and to determine the expected excitations processes. For the sake of simplicity we split the potential diagram into two potential diagrams. In Fig. 1(a) [1(b)] the gerade (ungerade) singlet states of H_2 are given, together with the excitation energies reachable with an even (odd) number of photons.

The excitation regions in the $\lambda=532$-nm experiment are at $5h\nu_{532}$ close to the $B\,^1\Sigma_g^+(v'=3)$-state, and at $6h\nu_{532}$ close to a set of states: $GK\,^1\Sigma_g^+(v'=2)$, $H\bar{H}\,^1\Sigma_g^+$, $I\,^1\Pi_g(v'=0)$, and $J\,^1\Delta_g(v'=0)$. The energy region at $7h\nu_{532}$ is above the $v^+=3$ ionization potential, and between the H(1s) +H($n=2$), and H(1s) +H($n=3$) dissociation limit. Moreover, in this energy region there are possible resonances with higher rovibrational excited Rydberg states, which are degenerate with the ionization continuum. Relevant is only the excitation to Rydberg states with a vibrational quantum number higher than the highest accessible vibrational ionization channel, i.e., $v\geq 4$; otherwise ionization would prevail.

In the $\lambda=355$-nm experiment there is only one excitation region that is not degenerated with the ionization continuum, namely, at $4h\nu_{355}$ with the same set of states as the $6h\nu_{532}$-energy region: $GK\,^1\Sigma_g^+(v'=2)$, $H\bar{H}\,^1\Sigma_g^+$, $I\,^1\Pi_g(v'=0)$. The energy region at $5h\nu_{355}$ is above the $v^+=9$ state, and between the H(1s)+ H($n=4$) and H(1s)+H($n=5$) dissociation limit. In the $5h\nu_{355}$-energy region it is again possible to excite bound Rydberg states.

In this case only $v \geq 9$ vibrational levels of Rydberg states can be excited.

Also in the $\lambda = 266$ nm experiment there is only one excitation region that is not degenerated with the ionization continuum, namely at $3h\nu_{266}$, with a set of states $B\,^1\Sigma_u^+(v'=23,24)$, $C\,^1\Pi_u(v'=7)$, $B'^1\Sigma_u^+(v'=1)$, and $D\,^1\Pi_u(v'=0)$. Four photons have already an energy that is above the $H(1s)+H^+$ dissociation limit. In this case, no resonances with bound Rydberg states are present.

In the above considerations concerning the excitation regions, nothing is mentioned about the excitation of doubly excited states. Since these states are repulsive

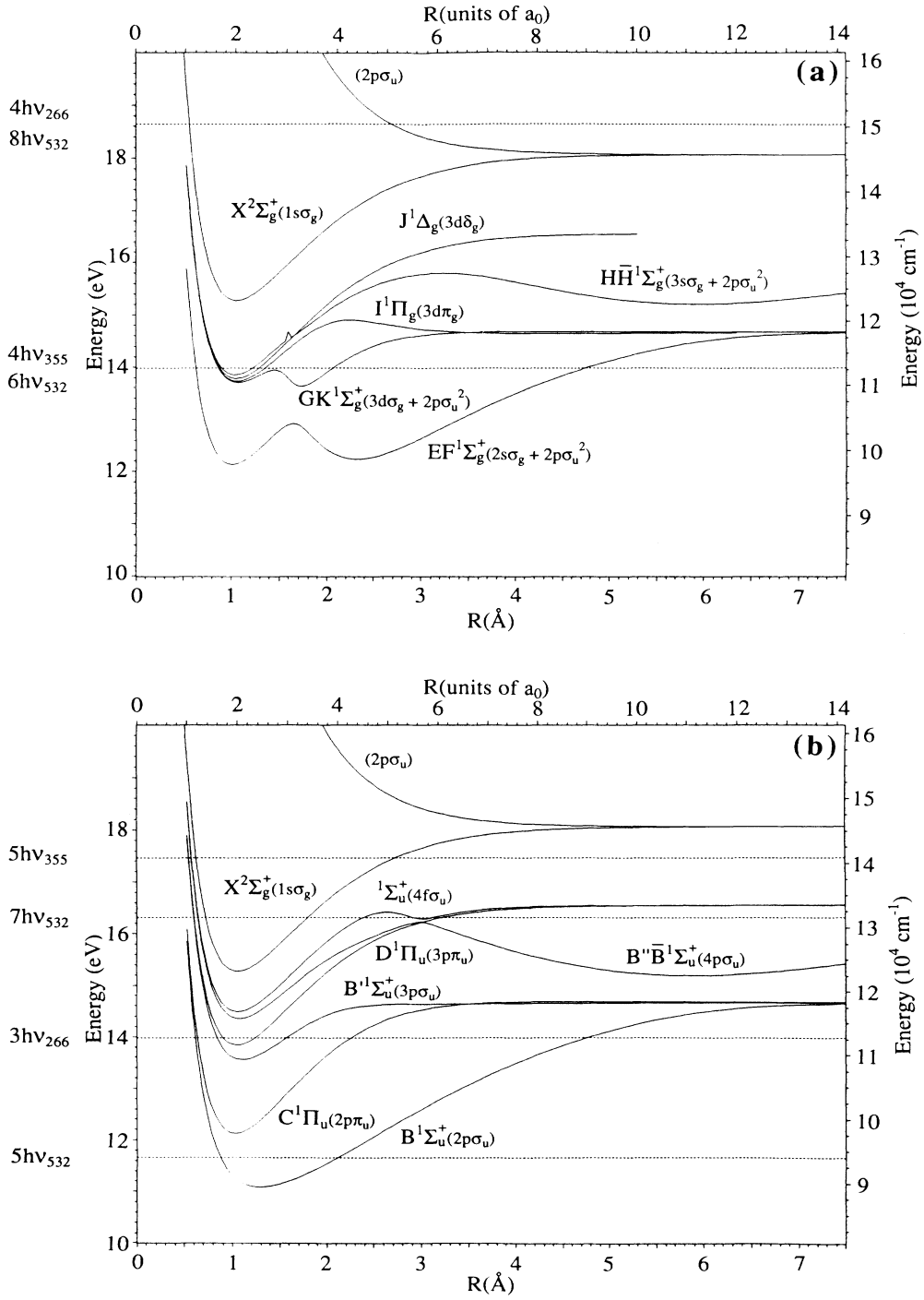

FIG. 1. (a) Potentials of the *gerade* singlet states of H_2, and the different excitation regions accessible with an *even* number of photons for the indicated wavelengths. (b) Potentials of the *ungerade* singlet states of H_2, and the different excitation regions accessible with an *odd* number of photons for the indicated wavelengths.

states, only excitation to the dissociation continuum can be performed. Such an excitation is not critical on the excitation energy. Therefore only the relative positions of the excitation regions with respect to the various dissociation limits are indicated. For the excitation of a doubly excited state an intermediate resonance is necessary to overcome a direct two-electron excitation. As a consequence, excitation of a doubly excited state is only of importance after resonance with an intermediate state at the energy regions around $6,7,8h\nu_{532}$, $5,6h\nu_{355}$, and $4h\nu_{266}$. The possibility to excite a doubly excited state depends strongly on the character of the intermediate resonance. An intermediate with a $2p\sigma_u$ electron enhances excitations to the lowest doubly excited states in a single-electron excitation. This condition is fulfilled for the $B\ ^1\Sigma_u^+$ state, which has a $2p\sigma_u$ electron, and for the double minimum state $GK\ ^1\Sigma_g^+$ and $H\bar{H}\ ^1\Sigma_u^+$, which have both partially $^1\Sigma_g^+(2p\sigma_u)^2$ character. Multiphoton excitation of doubly excited states via various vibrational levels of the $B\ ^1\Sigma_u^+$ state is reported by Verschuur *et al.*[18,19] Multiphoton excitation to doubly excited states via various vibrational levels of the lowest member of the double minimum states, the $EF^1\Sigma_g^+$ state, is reported by Buck *et al.*[20]

IV. RESULTS AND DISCUSSION

Photoelectron energy spectra recorded at wavelengths $\lambda=532$, 355, and 266 nm are presented in Figs. 2, 5, and 6, and discussed in separate paragraphs. For each wavelength two photoelectron energy spectra are given, recorded at different intensities. For the relevant ionization step the energies of the photoelectrons and the Franck-Condon factors of the ionization are given in the form of simulated spectra. The peak heights of the ATI peaks are taken equal to the normal ionization peaks for these spectra.

Before the photoelectron energy spectra are discussed, first a few remarks are made about the spectra themselves. The high limit intensity not only affects molecular processes, but also has its influence on the energy of the photoelectrons; see e.g., Ref. 21. The energy of the photoelectron peaks can be shifted due to the ac Stark shift of the ground state of the molecules H_2 and H_2^+, or due to the ac Stark shift of the excited electronic state of the H atom after dissociation. The shifts of intermediate states are not directly observed in the spectra. The shift of the ground state is estimated by the value of the dc Stark shift (i.e., in the limit for $E_{h\nu}\rightarrow 0$), which is equal to the product of the dc polarizability α of the ground state and the light intensity I. This estimation is valid when the photon energy is small compared to the energy of the first excited state. The polarizability of the ground state H_2 is $\alpha_{H_2}=5.417a_0^3$.[22] The polarizability of the ground state of H_2^+ is $\alpha_{H_2^+}=5.56a_0^3$.[23] The dc Stark shifts are therefore given by

$$\Delta E_{H_2}(\text{meV})=\alpha_{H_2}I=4.2I(10^{12}\text{W/cm}^2) \tag{1}$$

and

$$\Delta E_{H_2^+}(\text{meV})=\alpha_{H_2^+}I=4.3I(10^{12}\text{W/cm}^2)\ , \tag{2}$$

respectively. The shift of the photoelectron energy is only determined by the difference of the ac Stark shift of the molecular ground state, and the ionic ground state. For the intensities used in this experiment this difference is smaller than 6 meV, and therefore not observable in the measured spectra. The dc polarizability α_H of the ground state of the H atom is $\alpha_H=4.5a_0^3$,[22] which leads to ac Stark shifts smaller than 220 meV, for the intensities used. Evidently, the H^+ ion shows no ac Stark shift. The ac Stark shift of excited states of the H atom after dissociation cannot be estimated by the dc Stark shift. Unfortunately, a calculation of the first-order ac Stark shift also turns out to fail for the intensities of interest. On basis of these calculations, we expect a significant broadening of the photoelectron peaks, but we are not able to give reliable estimates. The strong radiation field is not only affecting the molecular ion, but also the otherwise free electron. Due to the oscillating electric field the electron is quivering, resulting in an additional term added to the directed kinetic energy. The quiver energy is in atomic units given by

$$E_{\text{quiver}}=\frac{I}{4\omega^2}\ , \tag{3}$$

where ω is the photon energy. The quiver energy of the electron after ionization is recovered when it leaves the laser focus adiabatically. Note that the quiver energy of the electron is not recovered in the case of a nonadiabatic separation of the electron and the field. This can lead to some extra asymmetric broadening of the photoelectron energy peaks. For the experiments reported here, the quiver energy of the electron is largest in the case of the $\lambda=532$ nm excitation at an intensity of $I=5.3\times10^{13}$ W/cm^2, taking the value $E_{\text{quiver}}=1.3$ eV. However, since the pulse duration is long compared to the time in which an electron leaves the laser focus, this shift will not affect the spectra. Only an imperfect cancellation of the ac Stark shift and the so-called ponderomotive shift will broaden the peaks, but this is a small fraction of the quiver energy. The energy broadening of the atomic photoionization peaks is determined by the ac Stark shift of the excited fragments after dissociation. The ac Stark shift of the H_2 ground state relative to the ac Stark shift of the excited fragment leads to a change of the dissociation energy, and thus the kinetic energy of the fragments. Another way of stating this is that the relative dissociation limits shift by the difference of the ac Stark shift of the ground state of the molecule and the ac Stark shift of the corresponding excited level of the fragment. The ionization process of the excited fragment starts from ac Stark-shifted excited level, instead of from the ground state. The ac Stark shift of an excited fragment is expected to be larger, compared to the shift of the ground state, since the photon energy is comparable to the energy distance between excited states. Therefore the asymmetric energy broadening in the photoelectron energy spectra is also expected to be larger. In the subsections below, the broadening of these excited states after dissociation will be discussed. Also, the influence of the ac Stark shifts of

excited states of H_2 on the resonant enhanced ionization process will be discussed.

A. $\lambda = 532$ nm results

The photoelectron energy spectra recorded at a wavelength of $\lambda = 532$ nm are presented in Figs. 2(a) and 2(b) for the intensities $I = 1.4 \times 10^{13}$ W/cm^2 and $I = 5.3 \times 10^{13}$ W/cm^2, respectively. The spectra are characterized by broad peaks. In Fig 2(b) no less than five ATI peaks are observed, and an indication of a sixth peak. The peaks show no structure, and the shape of the peaks differs negligibly from a Gaussian shape. The full width at half maximum is $\Gamma_{\mathrm{FWHM}} = 1.1$ eV, which is about half the photon energy $E_{h\nu} = 2.33$ eV. The center of the first peak is positioned at 2.2 eV. A very important point is that the spacing between the centers of the ATI peaks is not equal to the photon energy as expected on the basis of earlier atomic ATI experiments. The energy distance observed between the peaks is constant, but 330 meV smaller than the photon energy ($E_{h\nu} = 2.33$ eV). This effect is not the result of an error in the energy calibration. In Fig. 3 the energy difference between the excitation energy above $X\,^2\Sigma_g^+(v^+ = 0)$ and the observed electron energy is given as a function of the excitation energy above the $X\,^2\Sigma_g^+(v^+ = 0)$ state; i.e.,

$$[nh\nu_{532} - E(X\,^2\Sigma_g^+(v^+ = 0))] - E^m_{\mathrm{expt}} , \tag{4}$$

with $n - m = 8$, is given as a function of

$$nh\nu_{532} - E(X\,^2\Sigma_g^+(v^+ = 0)) , \tag{5}$$

where n is the number of absorbed photons, and m denotes the m^{th} electron peak in the experimental spectrum. A normal ATI spectrum, as observed in atoms, would lead to a horizontal line in Fig. 3, corresponding to a constant ionization potential. The first electron peak is not on the straight line, probably either due to ponderomotive effects (a not completely recovered quiver energy), or due to the presence of space charge. The energy given (4) is the energy that is left in the molecular ion in the form of rovibrational energy. The corresponding vibrational quantum numbers are indicated on the right-hand vertical axis of Fig. 3. The vibrational levels given at the most right-hand are accessed with one photon more, or one photon less. The line with nonzero positive slope indicates that with increasing energy of the photoelectron, the center of the ionic vibrational population is shifted to higher v^+ values. The broad and unstructured peaks are an indication of a smooth distribution over the various vibrational levels of the ionic ground state. Apparently, dissociation does not contribute to the spectrum. Elec-

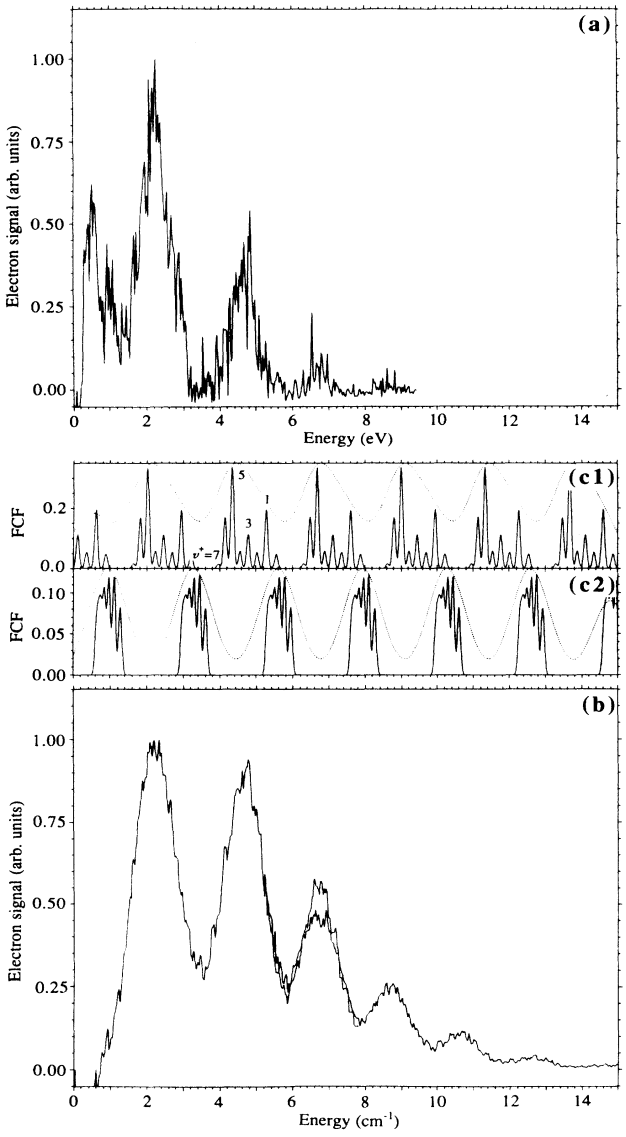

FIG. 2. Photoelectron energy spectra recorded at a wavelength of $\lambda = 532$ nm, with an intensity of (a) $I = 1.4 \times 10^{13}$ W/cm^2 and (b) $I = 5.3 \times 10^{13}$ W/cm^2. Between the two experimental spectra, two spectra and are presented that represent Franck-Condon factors (FCF) of the molecular ionization in an unperturbed situation (c1), and a perturbed situation (c2), as is illustrated in Fig. 4 (see text for explanation).

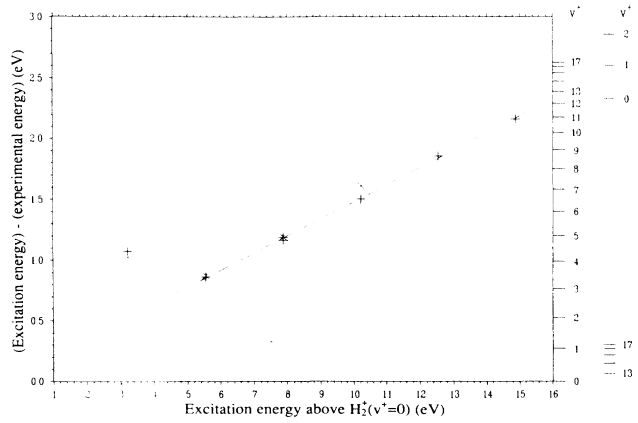

FIG. 3. Energy difference between the excitation above $v^+ = 0$ and the observed electron energy as defined by (4), i.e., vibrational energy of ionic ground state, as a function of the excitation energy above $v^+ = 0$ of the ion, as defined by (5).

tron peaks resulting from ionization of excited fragments appear at other positions than the observed peaks.

As can be seen from Fig. 1(b), the $B\,^1\Sigma_u^+(v'=3)$ state is the lowest resonance state, and is accessible with five photons. In order to explore the effect of the $B\,^1\Sigma_u^+(v'=3)$ state resonance on the photoionization electron spectra, a simulated spectrum is given in Fig. 2, convoluted with Gaussians of different widths, $\Gamma_{\rm FWHM}=0.1$ and 1.1 eV. These values are taken equal to the observed widths. This spectrum represents the Frank-Condon factors of the transition from the unperturbed $B\,^1\Sigma_u^+(v'=3)$ to the various vibrational ionization continua. The other simulated spectrum is the result of a calculation including laser intensity effects; this will be discussed later on. The ionization signal can be affected by resonances after absorption of six photons from the ground state, or one photon from the $B\,^1\Sigma_u^+(v'=3)$ state, namely, with the $GK\,^1\Sigma_g^+(v'=2)$, $H\bar{H}\,^1\Sigma_g^+(v'=0)$, $I\,^1\Pi_g(v'=0)$, and $J\,^1\Delta_g(v'=0)$ states. From the observed electron-energy spectrum we conclude that none of these states contributes directly to the observed ionization spectrum. A calculation of the Franck-Condon factors of these states to the various vibrational ionization channels results in a different spectrum, enhancing ionization into the lower vibrational channels. However, the $GK\,^1\Sigma_g^+$ state and the $H\bar{H}\,^1\Sigma_g^+$ state play a secondary role in the ionization process, due to their partially doubly excited character, as we will see later.

The effects of the intense radiation field on the molecule are taken into account by using the dressed-state formalism; the radiative (dipole) couplings are described by electronic couplings. We propose that via the intensity-dependent couplings between dressed states, adiabatic states are formed that play a dominant role in the observed shift of the Franck-Condon distribution. The intermediate state and the ionic ground state are dominantly perturbed by couplings to states which are dressed by one photon. We are aware of the fact that states that are dressed by more than one photon can have a significant contribution to the coupling. We therefore do not claim to give a full explanation, but rather a preliminary qualitative one. The coupling strength is proportional to the dipole moment between the two states involved, and proportional to the amplitude of the electric field of the radiation. The dipole moment between the doubly excited states and the $B\,^1\Sigma_u^+$ state is large. The doubly excited character $^1\Sigma_g^+(2p\sigma_u)^2$ of the $GK\,^1\Sigma_g^+$ state and the $H\bar{H}\,^1\Sigma_g^+$-state, dressed with one photon, is expected to couple most strongly with the $B\,^1\Sigma_u^+$-state. The bound ionic ground state $1s\sigma_g$ can only be coupled to the dressed repulsive ionic ground state $2p\sigma_u$. A calculation is performed on these sets of states, constructing adiabatic potentials and new vibrational wave functions denoted with quantum numbers v_a' and v_a^+. The coupling matrix elements are given by Bandrauk and Sink:[12]

$$H_{12}=\mu_{12}\sqrt{I}\ , \tag{6}$$

where μ_{12} is the dipole moment, which we gave the value of 0.3 a.u. The adiabatic construction of the potentials is presented in Fig. 4. The calculation is performed with a

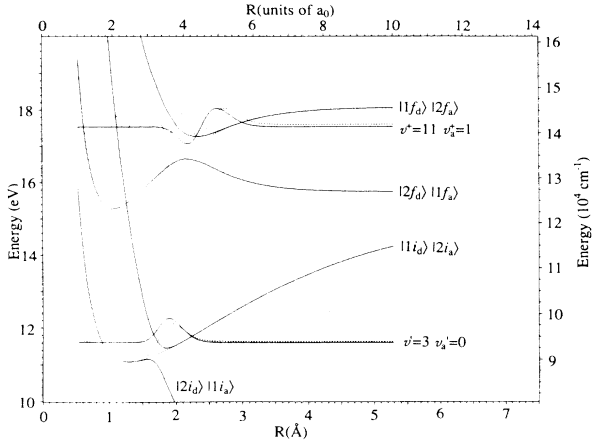

FIG. 4. Two sets of adiabatic potentials $|1i_a\rangle$, $|2i_a\rangle$, and $|1f_d\rangle$, $|2f_d\rangle$, constructed from the dressed $^1\Sigma_g^+(2p\sigma_u)(2p\sigma_u)$ state ($|2i_d\rangle$) coupled to the $B\,^1\Sigma_g^+$ state ($|1i_d\rangle$), and the dressed $(2p\sigma_u)$ state ($|2f_d\rangle$) coupled to the $X\,^2\Sigma_g^+$ state ($|1f_d\rangle$), respectively. Also some vibrational wave functions in both representations are drawn.

maximum value of $H_{12}=324$ meV, corresponding to an intensity of $I=5\times10^{13}$ W/cm^2. The coupling is localized around the crossing point of the two states involved, as at that point the two states, which are coupled by a single photon, are degenerate. We therefore took a Lorentz function for $H_{12}(R)$ with its maximum value at the crossing point.

A $v_a'=0$ wave function is calculated in the upper adiabatic potential, near the excitation energy. This $v_a'=0$ level is populated via the $v'=3$ level of the $B\,^1\Sigma_u^+$ state, since the Franck-Condon region of the ground state does not extend to the large internuclear distances of the $v_a'=0$ level. A Landau-Zener–type calculation of the transition probability at the crossing of the two potentials shows that the probability of passing the crossing diabatically is about 50%; a situation that is called intermediate coupling. In the adiabatic ion potential, vibrational wave functions are constructed, and denoted by v_a^+. A calculation of the Franck-Condon factors of the $v_a'=0$ level to the various vibrational ionization channels v_a^+ is presented in Fig. 2 in the form of a simulated spectrum. The Gaussian convolution of the electron peaks is again taken with a width of $\Gamma_{\rm FWHM}=0.1$ and 1.1 eV. The high-energy peaks are now at the right-hand position, while the lower-energy peaks are explained by an unperturbed $B\,^1\Sigma_u^+(v'=3)$ resonance and the unperturbed ionic state. The intermediate peaks are the result of a mixture of the diabatic and the adiabatic treatment. In the explanation we assume that the yield of the low-energy peaks is dominated by ionization at low intensities, while the electron peaks at higher energies are the result of ionization at higher intensities.

The calculations are just two extreme cases to illustrate the ionization process. To treat simultaneously the diabatic resonance and the adiabatic resonance due to a coupling with dressed states one has to calculate coupled Schrödinger equations as a function of the coupling strength, and integrate over all possible couplings in-

duced by the radiation field. Such a calculation is beyond the scope of this paper. In the above explanation, the coupling of the $B\ ^1\Sigma_u^+$-state to other dressed states, which are dressed by more than one photon, is not taken into account, although the observation of five ATI peaks in the electron-energy spectrum indicates that also dressed states with more than one photon can have a significant contribution. A treatment, which takes into account all dressed states goes beyond the scope of this paper.

B. $\lambda=355$ nm results

The photoelectron energy spectra recorded at $\lambda=355$ nm are presented in Figs. 5(a) and 5(b) for the intensities $I=1.5\times10^{13}$ W/cm^2 and $I=4.4\times10^{13}$ W/cm^2, respectively. The Franck-Condon factors of the transition from

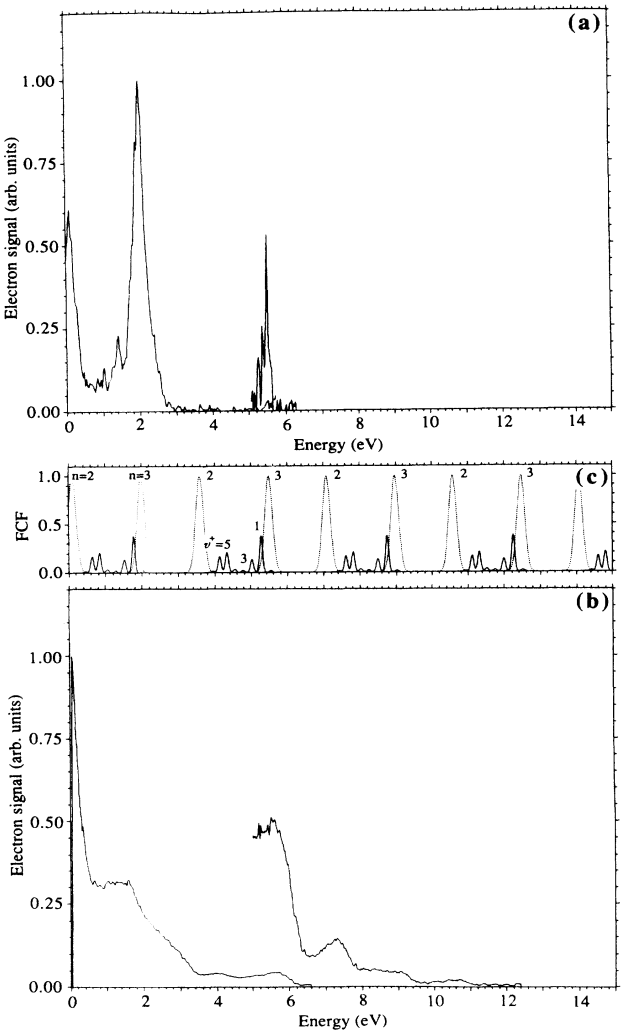

FIG. 5. Photoelectron energy spectra recorded at a wavelength of $\lambda=355$ nm, with an intensity of (a) $I=1.5\times10^{13}$ W/cm^2 and (b) $I=4.4\times10^{13}$ W/cm^2. The right-hand side of the spectra are expanded, but are measured at the same intensity. Between the experimental spectra a calculated spectrum (c) is given. The solid curve represents molecular ionization Franck-Condon factors, and the dotted spectrum indicates the ionization peaks of the dissociated fragments (see text for explanation).

the $GK\ ^1\Sigma_g^+(v'=2)$ state to the various vibrational ionization continua are represented by the solid line in the simulated spectrum. The other possible resonances at four-photon energy, i.e., $H\bar{H}\ ^1\Sigma_g^+(v'=0)$, $I\ ^1\Pi_g(v'=0)$, and $J\ ^1\Delta_g(v'=0)$ have the $v'=0$ vibration in common. Ionization of these $v'=0$ resonant states is exclusively a $\Delta v=0$ transition, since the lower part of these potentials deviates negligibly from the ionic ground-state potential. The Franck-Condon calculations of the molecular ionization via the possible intermediate resonances other than $v'=0$ states do not represent the measured spectra. Therefore, we conclude that the spectrum is dominated by ionization of the excited dissociation fragments and/or ionization via $v'=0$ states. Ionization of the dissociated fragments H($n=2$) and H($n=3$) is indicated by the dashed spectrum. The dissociation is dominantly to the H($1s$)+ H($n=2$) and H($1s$)+ H($n=3$) limits, as can be seen from a comparison between the simulated spectrum and the experimental one.

The already mentioned $GK\ ^1\Sigma_g^+$ state is a double minimum potential. The excited $v'=2$ vibrational level has its expectation value of the internuclear distance near the local maximum of the potential. The $v'=2$ level has both Rydberg character and doubly excited character. This is reflected in the bimodal structure of the calculated ionization signal (see Fig. 5). The observed ionization spectrum shows ionization to the lower vibrational levels ($v^+=0,1,2$). Only the inner part of the $v'=2$ vibrational wave function contributes to molecular ionization. The outer part of the wave function results in dissociation. The fact that the vibrational wave function extends to large internuclear distances is one of the two conditions to have a high probability to excite doubly excited states. The other condition is also fulfilled; namely, that the electronic character of the state allows a one-electron transition to a doubly excited state with a $(2p\sigma_u)$ core. The electronic character of the $GK\ ^1\Sigma_g^+(v'=2)$ state is for a substantial fraction $^1\Sigma_g^+(2p\sigma_u)^2$, due to the large electronic coupling between the $Q_1\ ^1\Sigma_g^+(2p\sigma_u)^2$ state and the Rydberg state $E\ ^1\Sigma_g^+(1s\sigma_g)(2s\sigma_g)$ and $G\ ^1\Sigma_g^+(1s\sigma_g)(3d\sigma_g)$.[24] This explains, the dissociative character of the multiphoton process resonant via the $GK\ ^1\Sigma_g^+(v'=2)$ state.

In case of dissociation the ac Stark shifts of the H($n=2$) and H($n=3$) states are of importance, since the H atom is created in an excited state inside a strong radiation field. Analogous to the shift of the ground state, the shift of the excited state of the atom after dissociation is not recovered in the ionization process, and results in an asymmetric broadening of the electron peak. As mentioned before, in the case of molecular ionization via $v'=0$ states broadening is expected to be small because of the small difference in molecular and ionic ac Stark shift. In both cases, molecular and atomic ionization, shifts to lower energies are unexpected and suggest a possible role of space charge.

C. $\lambda=266$ nm results

The photoelectron energy spectra recorded with a wavelength of $\lambda=266$ nm are presented in Figs. 6(a) and

6(b) for the intensities $I=1.5\times10^{12}$ W/cm^2 and $I=5.3\times10^{12}$ W/cm^2 respectively. In Fig. 6(b), a part of a spectrum recorded at an intensity of $I=1.2\times10^{13}$ W/cm^2 is presented. These spectra show the most distinct structure, in particular, the spectrum of Fig. 6(a). The best resolved structure can be assigned to vibrational ionization continua, as indicated in the simulated spectrum. The highest peaks correspond to ionization into the $v^+=1$ and $v^+=7$ channels, both with some satellite peaks ($\Delta v\neq0$ transitions). In the spectrum recorded at a higher intensity [Fig. 6(b)], the peaks become broad, and the satellite peaks become unresolved, but the center of the peaks remains at the position of the $v^+=1$ and $v^+=7$ peaks. In the high-intensity spectrum, new peaks

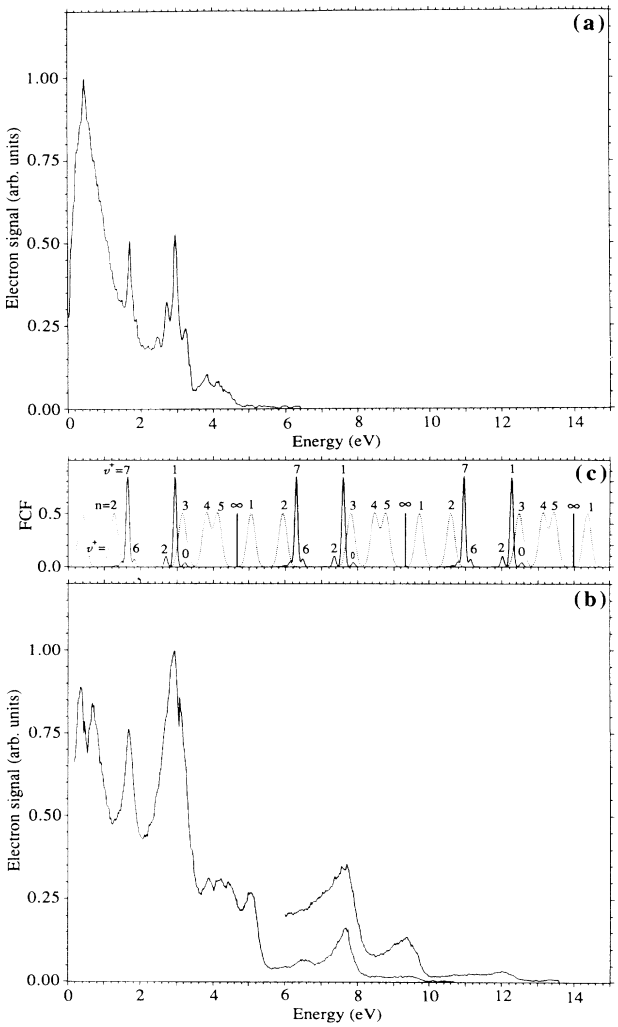

FIG. 6. Photoelectron energy spectra recorded at a wavelength of $\lambda=266$ nm, with an intensity of (a) $I=1.5\times10^{12}$ W/cm^2 and (b) $I=5.3\times10^{12}$ W/cm^2, and $I=1.2\times10^{13}$ W/cm^2 (inset). Between the experimental spectra a calculated spectrum (c) is given. The solid curve represents molecular ionization Franck-Condon factors, and the dotted spectrum indicates the ionization peaks of the dissociated fragments (see text for explanation).

are also present at higher energies again assigned to the $v^+=1$ and $v^+=7$ ionization channels, but with an extra photon absorbed. This means that ATI is observed in molecular hydrogen ionized with $\lambda=266$ nm, as was the case with $\lambda=532$ nm. In the spectrum recorded at even higher intensities [additional curve in Fig. 6(b)] ATI peaks with two excess photons are present. Besides the signal assigned to the vibrational ionization continua also part of the signal can be assigned to dissociation of H_2. Dissociation into the H($1s$)+ H($n\geq4$) channels is clearly observed, of which the ionization of the H($n=4$) and H($n=5$) fragments is energetically resolved. Dissociation into the H($1s$)+ H($n=3$) channel may be present underneath the $v^+=0,1,2$ peaks. In the spectrum of Fig. 6(b) ionization of the ground-state fragment H($1s$) is observed also.

The Franck-Condon factors of the transitions from the $C\,^1\Pi_u(v'=7)$ state and the $B\,^1\Sigma_u^+(v'=1)$ state to the various vibrational ionization continua are given in Fig. 6 in the form of the simulated spectrum. These states are resonant with three photons, as are the $D\,^1\Pi_u(v'=0)$ state and the $B\,^1\Sigma_u^+(v'=23,24)$ state. The $D\,^1\Pi_u(v'=0)$ state can have a contribution to the $v^+=0$ ionization continuum, but is not explicitly indicated in the simulated spectrum. The ionization is a pure $\Delta v=0$ transition, due to the Rydberg character of the $D\,^1\Pi_u$ state. The $B\,^1\Sigma_u^+(v'=23,24)$ state does not contribute to the ionization process, but we have a contribution in the dissociation process. As can be seen from Fig. 6(a) and the simulated spectra, the main contributions to the ionization process are resonances via the $C\,^1\Pi_u(v'=7)$ state and the $B\,^1\Sigma_u^+(v'=1)$ state. The dashed spectrum represents again ionization of the excited fragments. Besides ionization of the excited $H(n)$ fragment with $n\geq2$, ionization of the H($1s$) fragment by three photons is observed also. For the first time, photoionization of both fragments after a photodissociation process is observed in a photoelectron energy spectrum.

In the $\lambda=266$ nm results the electronic coupling of dressed states with the intermediate states plays a minor role in the excitation process. The observed spectrum is fairly well explained by the unperturbed resonances. The minor influence of dressed states can be explained by the fact that only doubly excited states and the ionization continuum can contribute to the perturbation. The coupling of the intermediate states with the doubly excited states is small due to the character of the doubly excited states.

D. General discussion

In general, the observed photoelectron energy spectra are explained by the presence of intermediate resonances in the multiphoton excitation scheme, for all wavelengths used. The character of the intermediate resonances is determined by couplings between molecular eigenstates and dressed states. The influence on the ionization process of these couplings is most clearly present in the $\lambda=532$ nm results. This is due to the fact that only in the case of excitation with $\lambda=532$ nm, the intermediate state couples to a dressed state which lies below the ionization limit. In addition, the maximum light intensity was

higher for this wavelength than for the other two wavelengths. The $\lambda=355$ nm spectra and the $\lambda=266$ nm spectra are explained in terms of photoionization or photodissociation of unperturbed intermediate states. Although couplings of dressed states with the intermediate states do not show up in the photoelectron spectrum, the couplings cannot be neglected. The shift of the molecular levels in the radiation field is due to the radiative couplings between dressed states, which are essential to shift the intermediate state into resonance.

The influence of the radiation field on the photoelectron energy spectra can also be described in another perspective. The quiver motion of the electron during ionization has a polarizing effect on the H_2^+ core. These polarizing forces affect the binding energy of the H_2^+, the potential, and therefore the vibrational wave functions. The α_0 parameter, which is defined by

$$\alpha_0 \equiv \frac{\sqrt{I}}{\omega^2} \tag{7}$$

in a.u., is the amplitude of the quiver motion. In the $\lambda=532$ nm spectrum α_0 takes the value of 5.3, which means that the electron oscillates over a distance of 5.6Å. This value is larger than the equilibrium distance of all potentials of H_2. Therefore it is not surprising that a coupling between the forced electron motion and the potential of the H_2^+ core exists. At ionization, the electron leaves a perturbed H_2^+ core, and takes the information of the perturbed H_2^+ core with it in the form of energy. The broadening of the ATI peaks in the $\lambda=532$ nm spectra is likely due to this mechanism. The α_0 values for the $\lambda=355$ nm results are at least a factor of 2.7 lower and the values for the $\lambda=266$ nm results are even at least a factor of 17 lower. The ATI part of the photoelectron energy spectra (i.e., photoelectron energies larger than the energy of one photon) of the $\lambda=355$ and 266 nm results is, in general, similar to the normal photoionization part of the spectrum.

A detailed explanation of the widths of the electron energy peak is still difficult, but a few general remarks can be made about additional broadening mechanisms. A possible guideline is that the peaks assigned to dissociation show all an asymmetric broadening, whereas the peaks assigned to the ionization of the molecule H_2 show a symmetric broadening. The ac Stark shift of the excited state of the fragment can have a significant influence on the broadening of the atomic ionization peaks. The widths of the molecular ionization peaks can be understood qualitatively by the shift of the ionic ground-state levels due to the radiative coupling with the dressed $2p\sigma_u$ state. The electron leaves a perturbed ion, and shows the information of the perturbation in its kinetic energy.

ACKNOWLEDGMENTS

We thank Professor J. Los for his valuable contributions in the discussions. This work is part of the research program of the Stichting voor Fundamenteel Onderzoek der Materie (Foundation for Fundamental Research on Matter) and was made possible by financial support from the Nederlandse Organisatie voor Wetenschappelijk Onderzoek (Netherlands Organization for Advancement of Research).

[1]P. Agostini, F. Fabre, G. Mainfray, G. Petite, and P. N. Rahman, Phys. Rev. Lett. **42**, 1127 (1979).
[2]P. Kruit, J. Kimman, H. G. Muller, and M. J. van der Wiel, Phys. Rev. A **28**, 248 (1983).
[3]D. Normand, C. Cornaggia, and J. Morellec, J. Phys. B **19**, 2881 (1986).
[4]C. Cornaggia, D. Normand, J. Morellec, G. Mainfray, and C. Manus, Phys. Rev. A **34**, 207 (1986).
[5]P. Bucksbaum (private communication).
[6]J. C. Miller and R. N. Compton, J. Chem. Phys. **75**, 22 (1981).
[7]J. Kimman, J. W. J. Verschuur, M. Lavollee, H. B. van Linden van den Heuvell, and M. J. van der Wiel, J. Phys. B **19**, 3909 (1986).
[8]J. W. J. Verschuur, L. D. Noordam, J. Los, P. Berger, A. Migus, and H. B. van Linden van den Heuvell (unpublished).
[9]D. Normand and J. Morellec, J. Phys. B **21**, L625 (1988).
[10]L. Bigio and E. R. Grant, J. Chem. Phys. **83**, 5361 (1985).
[11]L. Bigio, G. S. Ezra, and E. R. Grant, J. Chem. Phys. **83**, 5369 (1985).
[12]A. D. Bandrauk and M. L. Sink, J. Chem. Phys. **74**, 1110 (1981); A. D. Bandrauk and N. Gélinas, *ibid.* **86**, 5257 (1987).
[13]S.-I Chu, J. Chem. Phys. **75**, 2215 (1981).
[14]X. He, O. Atabek, and A. Giusti-Suzor, Phys. Rev. A **38**, 5586 (1988).
[15]C. Cohen-Tannoudji and S. Reynaud, J. Phys. B **10**, 345 (1977).
[16]M. A. Quesada, A. M. F. Lau, D. H. Parker, and D. W. Chandler, Phys. Rev. A **36**, 4107 (1987).
[17]P. Kruit and F. H. Read, J. Phys. E **16**, 313 (1983).
[18]J. W. J. Verschuur and H. B. van Linden van den Heuvell, Chem. Phys. **129**, 1 (1989).
[19]J. W. J. Verschuur, L. D. Noordam, J. H. M. Bonnie, and H. B. van Linden van den Heuvell, Chem. Phys. Lett. **146**, 283 (1988).
[20]J. Buck, D. H. Parker, and D. W. Chandler, J. Phys. Chem. **92**, 3701 (1988).
[21]P. Agostini, J. Kupersztych, L. Lompré, G. Petite, and F. Yergeau, Phys. Rev. A **36**, 4111 (1987).
[22]A. A. Radzig and B. M. Smirnov, *Reference Data on Atoms, Molecules, and Ions* (Springer-Verlag, Berlin), p. 444 for H_2, p. 119 for H.
[23]H. A. Stuart, in *Atom- und Molekularphysik*, Vol. 1 of *Landolt-Börnstein*, edited by A. Eucken (Springer-Verlag, Berlin, 1950), p. 401.
[24]L. Wolniewicz and K. Dressler, J. Chem. Phys. **82**, 3292 (1985).